ALMA Receiver Optics Design

A. Baryshev (SRON), M. C. Carter (IRAM), L. R. D'Addario (NRAO), B. N. Ellison (RAL), W. Grammer (NRAO), Y. Sekimoto (NRO), J. W. Lamb (Caltech)

1 Introduction

Since the establishment of the Joint Receiver Design Group (JRDG), the requirements for the frontend have been refined and several major design decisions made, as summarized in Section 2. Principally they prescribe a single dewar for all the receiver bands, and these bands will be realized as individually testable cartridges.

A Workshop was held in Tucson in September 2000 to define a layout for the optics and dewar. Section 3 lists the design goals for the Workshop, and the configuration that emerged is detailed in this document. This includes the overall arrangement, and the details of the optics of the individual Bands. These bands are those defined by Wootten *et al.* [1] and endorsed with minor adjustment for Band 3 by the ALMA Scientific Advisory Committee (ASAC) [2]. The design goals led to a natural division of the bands into three groups. Representative designs for the optics of each of these groups are given.

2 Previous Design Decisions

During the project there have been several major decisions which are documented here for completeness. Some of these significantly influence the layout of the optics. Major decisions are

1. All cryogenic components will be in a single dewar.
2. There will be three temperature stages in the dewar at ~70 K, 12 K, and 4 K.
3. Each receiver band (frequency range covered by a single set of components) will be contained in a cartridge that may be tested as a unit and inserted into the dewar without disturbing any other cartridges.
4. The water vapor radiometer will be operated in a separate package at ambient temperature. It therefore requires a pick-off mirror to put the beam within 10 arcsec of any of the observing beams.
5. There will be no cold load for receiver calibration. However, provision will be made for a cold load for the vapor radiometer.
6. There will be no quasioptical diplexers for sideband rejection. This is based on a compromise between sensitivity and complexity (reliability)
7. The different bands will share the focal plane so that no switching mirror is required to select a given frequency.

These decisions were influenced by both performance criteria and practical considerations. Testability and mass production by separate groups dictated that the different receiver bands should be constructed in individual cartridges that can be inserted into a single dewar. The major disadvantage of this is that the dewar is larger than it would be with a more integrated approach, but the advantages of being able to change and test individual bands was deemed to be worth this sacrifice.

3 Design Goals

Because of the large number of bands (10 dual-polarization), the wide frequency coverage (> 4 octaves), and the high sensitivity requirements needed to profit fully from the excellent site, the trade-offs between some of the parameters is not straightforward. In general those parameters which affect most of the observing modes (*e.g.*, sensitivity, reliability) were favored above parameters which were for more specialized modes (such as circular polarization). The physical complexity of the receiver dictated that practical issues had to be seriously considered. These trade-offs are discussed in the text.

The design goals are divided into two categories according to whether they are fundamental to the performance of the receiver, or related to the practicality of construction and maintenance. In some cases there may be conflicts between these goals, but wherever possible the sensitivity should not be compromised.

3.1 Practical Goals

1. Receivers will be interchangeable between antennas (no on site alignment)
2. Optics part of Rx — Fixed alignment between optics and dewar
3. Antenna mounting flange should be preset within tolerances
4. Cartridges interchangeable between dewars with no re-alignment required
5. Alignment sensitivity to thermal contraction minimized
6. Alignment insensitive to dewar deflections under vacuum
7. Alignment ensured by machining
8. Optics in cartridge where practical
9. Optics cold where practical
10. No moving parts
11. Flexible for future upgrades/clearly defined interfaces
12. Standardize designs among bands
13. Maximize reliability
14. Minimize costs

3.2 Performance Related Goals

1. Minimize window apertures (IR loading, RF loss minimized)
2. Horn aperture less than 10 wavelengths
3. Minimize added noise
4. Maximize aperture efficiency: Reduction < 5 % relative to ideal corrugated horn
5. Aberrations: < 1 %
6. Truncation loss: < 1 %
7. Dissipative losses: < 1 %
8. Scattering losses: < 1 %
9. Polarization loss: < 1 %
10. Polarization: Beam squint: < 1 % of FWHM

4 Design Details

4.1 Cartridge Designs

4.1.1 Cartridge Style A

Band 1 (31.3–45 GHz) is the most demanding in terms of size. The optical elements are too large to place in the dewar, so only the feed horn will be cooled. Re-imaging optics are needed to allow a reasonable size of horn, and achieve high efficiency that is essentially frequency independent. Two mirrors, one plane and one ellipsoidal, were considered but the folded geometry resulted in optics that were too large to fit in the space above the dewar. Using a corrugated horn and a lens results in a much more compact design. Since a design for Band 1 had already been developed for the prototype antenna evaluation receiver [3] this was used for Band 1 and scaled for Band 2.

Figure 1 gives the layout and dimensions for the Band 1 optics. It comprises a conical corrugated horn and an aspheric PTFE lens. The corrugated horn was designed using a mode-matching program to optimize the pattern and the return loss (shown in Figure 2). It has an aperture radius of 30 mm and an opening angle of 4.57°. To determine the lens focal length and location, a frequency independent design was used so that the position of the waist from the horn/lens would match the required antenna waist position. Since the lens is quite thick it has a significant dielectric loss, and its diameter was chosen to make the loss due to truncation and dissipation roughly the same at 1.5–2 %.

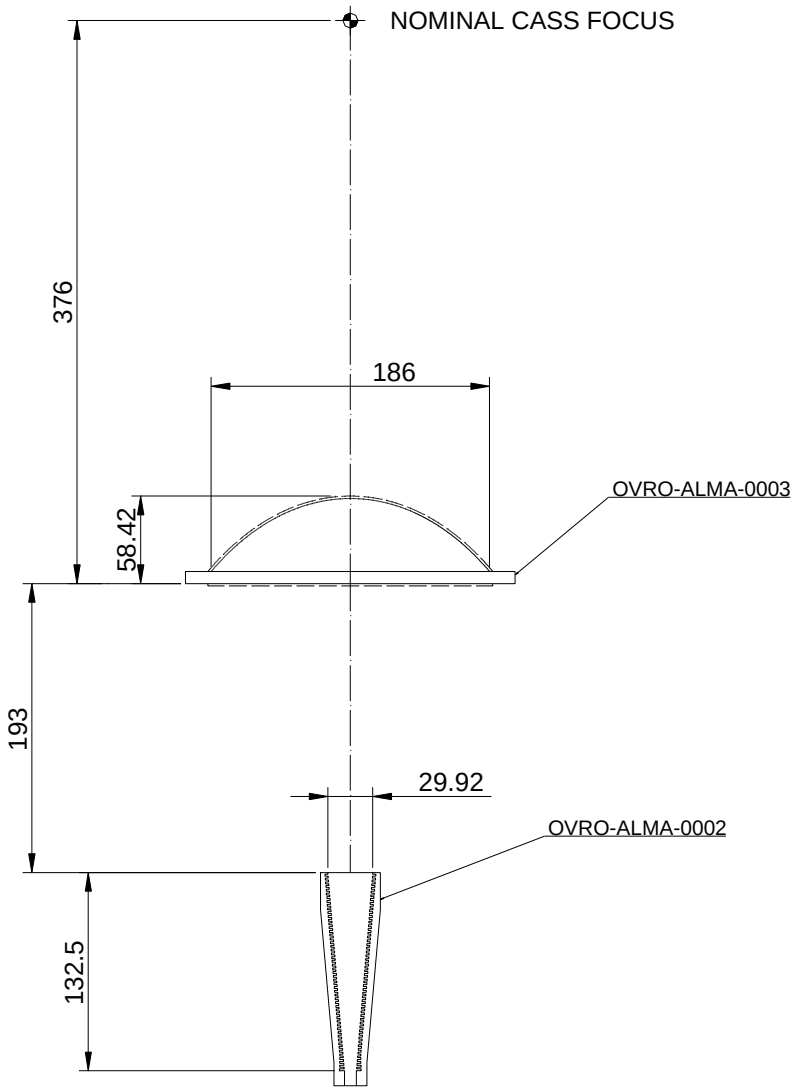

Figure 1: Band 1 optical design (will show IR filters and dewar wall).

Antireflection layers may be made by machining grooves in the surface. Straight grooves should be used on the flat surface of the lens, but this would be extremely difficult to do on the curved surface. Circular grooves can be used instead but those generate some cross-polarization and astigmatism. A viable alternative is to drill a regular array of holes into the surface, which is the choice for these lenses.

The lens is used as the vacuum window, which avoids an extra element in the optics. Since the truncation by the lens is at the level of a couple of percent, care has to be taken that the power not passing through the lens is terminated at ambient temperature.

Performance of the system was determined by calculating the antenna aperture field to find the aperture efficiency. Starting with the horn aperture field determined by mode-

matching, the field was propagated to the lens by integration. This field was traced through the lens by geometrical optics and a diffraction integral gave the distribution at the secondary mirror. Most of the contributions to efficiency are therefore accounted for, including: departures of the horn aperture field from the ideal $J_0(r)$ distribution; phase errors in the feed aperture; cross-polarization due to the feed; truncation loss at the lens, absorption in the lens; and blockage in the aperture plane. Losses which are not included are: reflection, scattering, and absorption in the filters; reflections at the lens surfaces; aberrations at the lens due to the phase center of the wave not being precisely at the focus; and losses due to the offset of the feed from the antenna axis. These were separately estimated.

Table I summarizes these various contributions. The feedhorn contribution was found by repeating the calculation with an idealized horn aperture field.

Because of the relatively small aperture of the lens, there is a perturbation of the pattern at the secondary due to edge diffraction. This appears mainly as a phase error which can be removed by refocusing the secondary mirror, which is assumed to be the case in the Table.

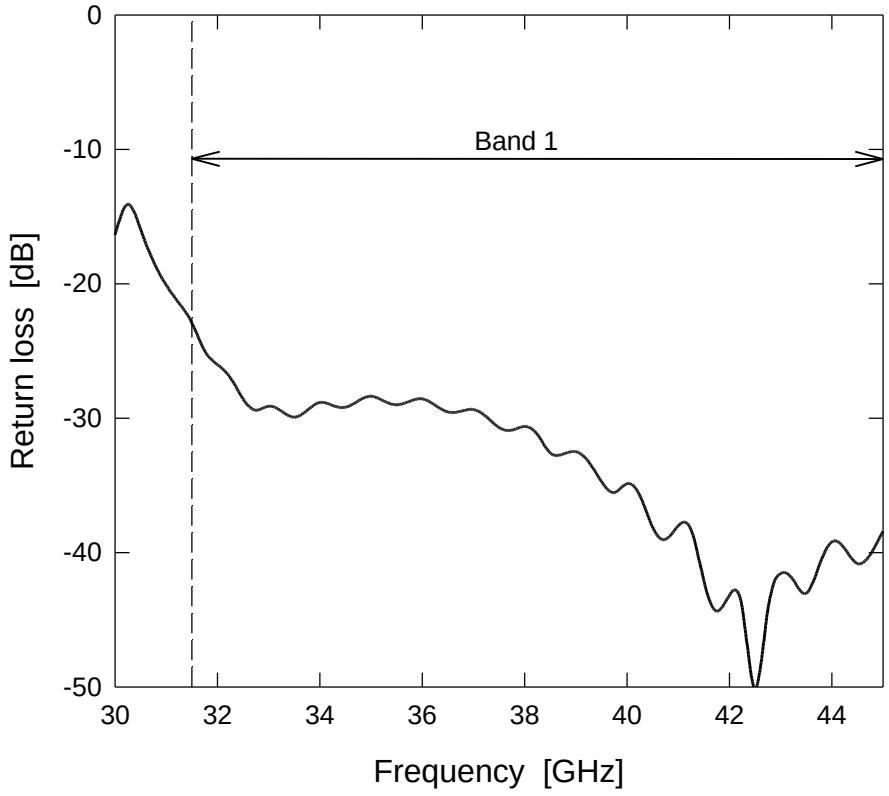

Figure 2: Return loss calculated for Band 1 corrugated horn.

TABLE I: ESTIMATED APERTURE EFFICIENCY LOSS AND ADDED NOISE FOR STYLE A CARTRIDGES

Band	Frequency [GHz]	Efficiency Loss [%]	Added Noise [K]
1	31.5	11.5	6.4
	38	8.5	8.7
	45	8.1	11.0
2	67	TBD	TBD
	81	TBD	TBD
	90	TBD	TBD

4.1.2 Cartridge Style B

Band 3 (84-116 GHz) and band 4 (125-164 GHz) are both Style B (Figure 3). External reflecting optics are used to produce a beam-waist close to the dewar wall to minimize the radiative heat load on the cryogenic system. A second focusing element is required inside the dewar since it is impractical to have the feed aperture very close to the dewar window. Since the cold optics are within the 140-mm diameter of the cartridge, it can easily be inserted into the dewar as a single unit. These cartridges occupy the outer circle at a diameter of 670 mm.

A plane mirror offset by 210 mm in the telescope focal plane reflects the incoming beam through an angle of 52° to an offset ellipsoidal mirror with a focal length of 87 mm. The ellipsoid reflects the beam through a 50° angle, making it parallel to the telescope axis, and produces a mid-band beam-waist of about 4.5 mm at the 24-mm diameter dewar window. After passing through an infrared filter anchored to the first stage shield of the dewar, the beam is imaged by a 60-mm focal-length lens on to a corrugated horn.

The corrugated horn supports both polarizations, which are separated in waveguide by an orthomode transducer.

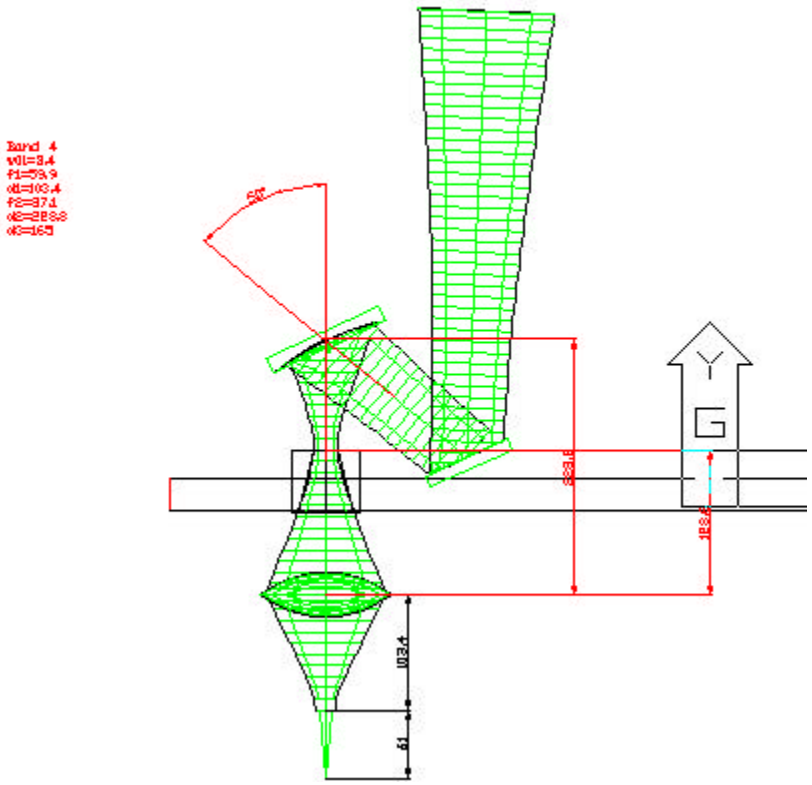

Figure 3: Layout and dimensions for Band 3 optics.

Table II lists the expected performance measures for Style B cartridges.

TABLE II: ESTIMATED APERTURE EFFICIENCY LOSS AND ADDED NOISE FOR STYLE B CARTRIDGES

Band	Frequency [GHz]	Efficiency Loss [%]	Added Noise [K]
3	84	TBD	TBD
	100	TBD	TBD
	116	TBD	TBD
4	125	TBD	TBD
	144	TBD	TBD
	163	TBD	TBD

4.1.3 Cartridge Style C

Style C cartridges include Bands 5–10. Internally, the optics vary among the cartridges according to the specific requirements, but they share some common features. For all the bands the antenna secondary focus is close to the dewar wall. All the imaging of the beam is done by cold reflective optics with 2 to 4 mirrors. Corrugated horns are the preferred beam-forming elements, but 'planar' structures such as twin-slot antennas on hyper-hemispherical will be considered. For the higher frequencies quasioptical polarizers and LO injection components may be required.

Optics for Band 6 are shown schematically in Figure 4.

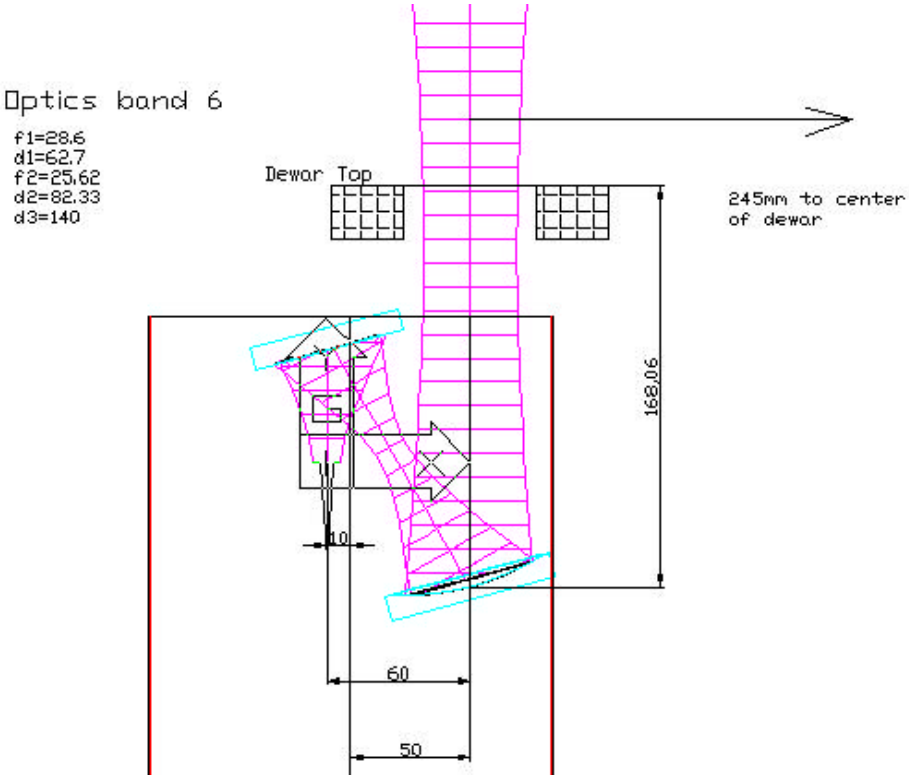

Figure 4: Optics layout and dimensions for Band 6.

Figure 5 presents the configuration for Band 7. The dewar window is radially offset by 130 mm from the dewar axis. The beam passing through the window and infrared filters is reflected through an angle of 116º by a plane mirror. It is then reflected by an ellipsoidal mirror where it is turned by 26º and focused onto a grid with a waist radius of about 2.4 mm. The grid separates the two linear polarizations, which are then incident on two identical ellipsoidal mirrors. They are then reflected down by 26º to converge into the corrugated horns by way of two flat mirrors.

Losses due to the beam distortion and cross-polarization are low due to the small incidence angles of the ellipsoidal mirrors.

Although it appears complex, this optical arrangement allows some flexibility in mixer design and LO injection.

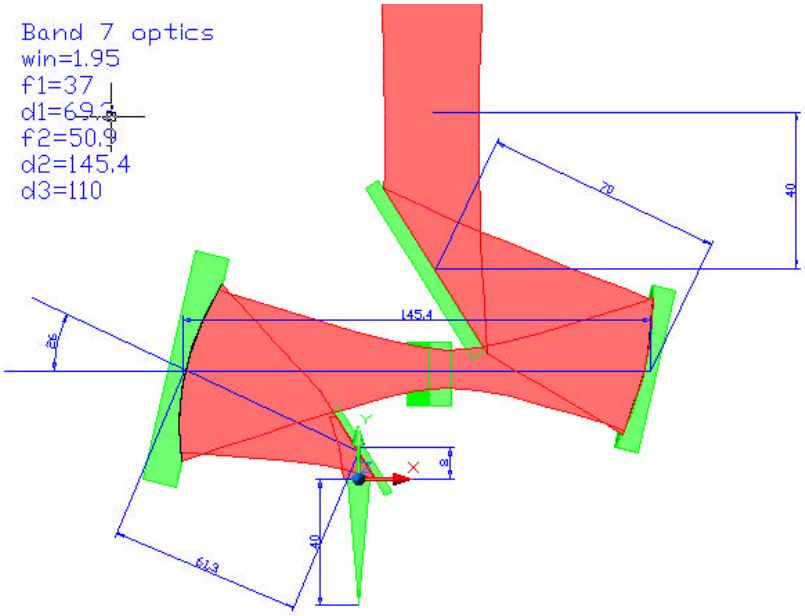

Figure 5: Schematic of the Band 7 optics configuration.

Band 9 optics are based on the optical design by van de Stadt for the FIRST HIFI receiver. The original design comprised two ellipsoidal (converging) mirrors with an intermediate hyperboloidal (diverging) mirror. The intention of this was to achieve significant cancellation of the distortion and cross-polarization of the individual mirrors according to known geometrical optics criteria. In adapting this to the ALMA receiver requirements, the hyperboloidal mirror was found to be close enough to a planar surface to omit entirely.

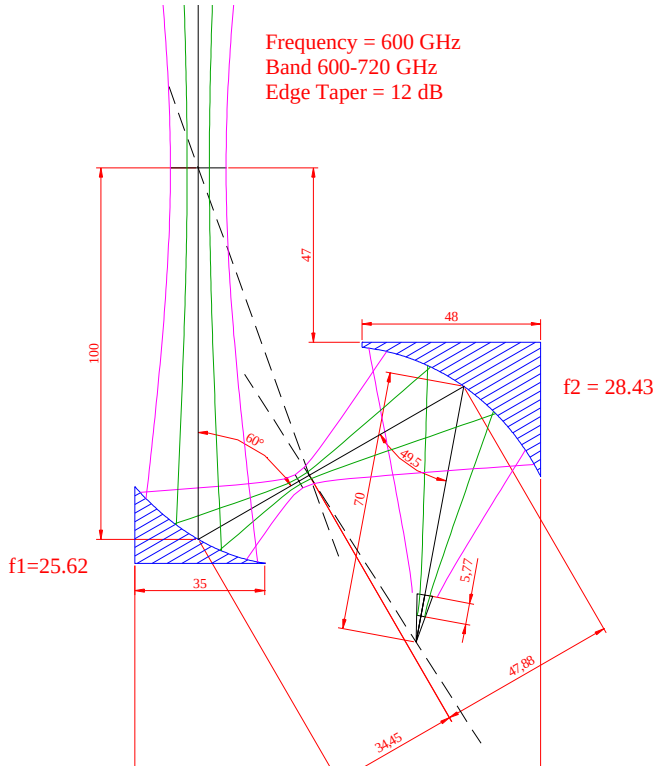

Figure 6: Optical scheme for Band 9 derived from the HIFI receiver optics concept.

For Bands 5–10 the expected performance measures are listed in Table III

TABLE III: ESTIMATED APERTURE EFFICIENCY LOSS AND ADDED NOISE FOR STYLE C CARTRIDGES

Band	Frequency [GHz]	Efficiency Loss [%]	Added Noise [K]
5	163	TBD	TBD
	187	TBD	TBD
	211	TBD	TBD
6	211	TBD	TBD
	243	TBD	TBD
	275	TBD	TBD
7	275	TBD	TBD
	323	TBD	TBD
	370	TBD	TBD
8	385	TBD	TBD
	442	TBD	TBD
	500	TBD	TBD
9	602	TBD	TBD
	661	TBD	TBD
	720	TBD	TBD
10	787	TBD	TBD
	868	TBD	TBD

950	TBD	TBD

4.2 Dewar Layout

A view of the cartridge locations is shown in Figure 7. The outer vacuum container of the dewar is 970 mm in diameter and 400 mm high. Ten cartridges may be accommodated in it, each containing a dual polarization receiver with an optical input, a waveguide LO input, co-axial IF outputs, and bias wiring. For cartridges with a diameter of 180 mm are located on the inner circle at a diameter of 300 mm for Bands 7–10. Bands 1, 2, 5, and 6 also utilize 180 mm diameter cartridges and are arranged on a 590 mm diameter circle. Cartridges with diameters of 140 mm located on a 670 mm circle house the remaining Bands, 3 and 4.

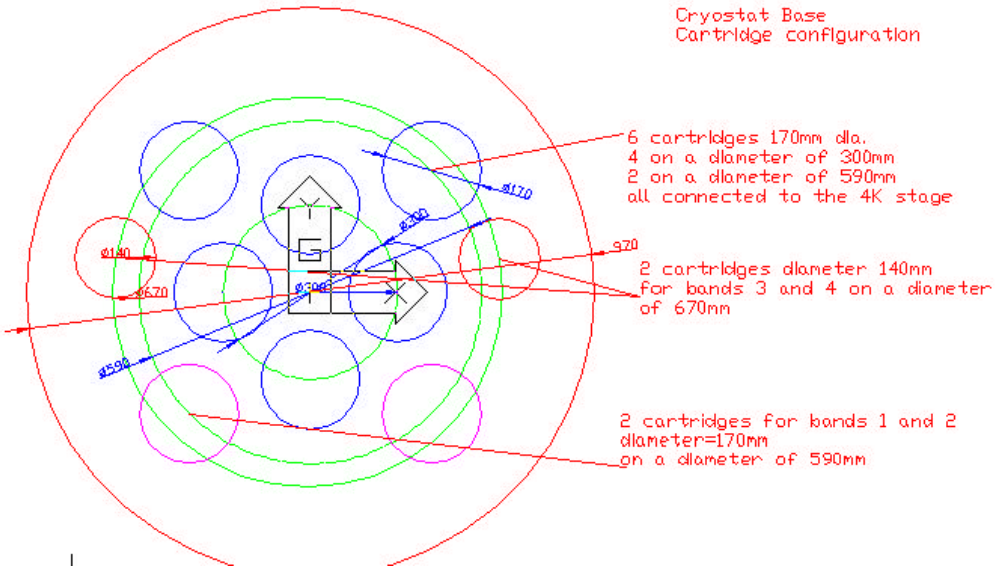

Figure 7: Locations of cartridges in dewar.

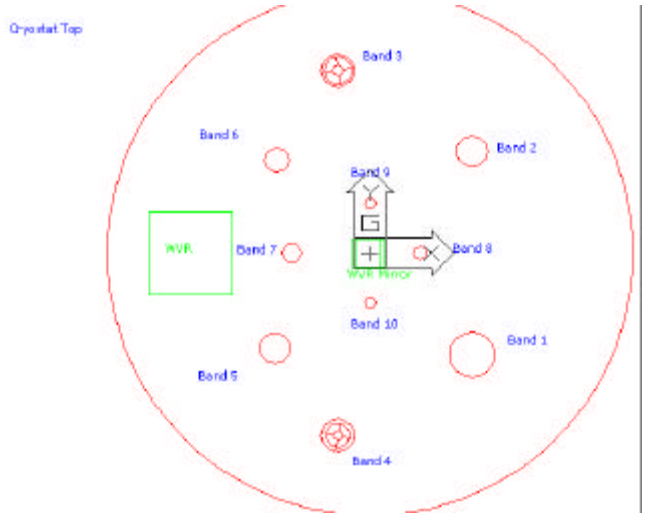

Figure 8: Arrangement of windows on the top of the dewar.

All of the cold optical elements are integral with the cartridges. As shown in Figure 8, the vacuum windows are directly above the cartridge axes for Bands 1–4. Windows for Bands 5–10, however, are offset towards the dewar axis by the folded optics in the cartridge.

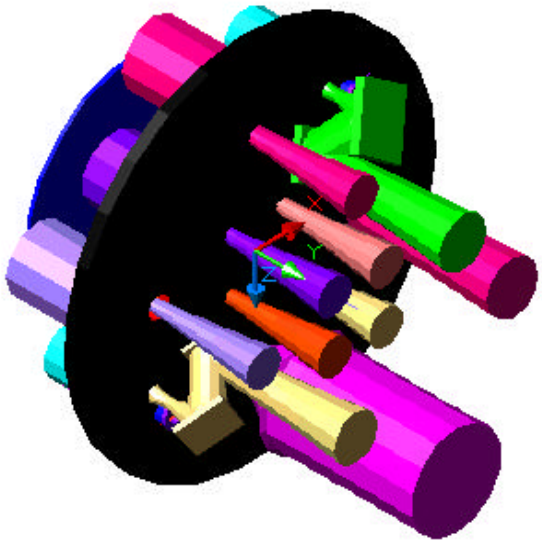

Figure 9: Layout of the optics showing the beams going into the dewar.

4.3 The Water Vapor Radiometer

The water vapor radiometer will be a self-contained unit with a pickoff mirror on the axis of the cryostat. This puts the WVR beam within 10 arcmin of any of the observing beams. This pickoff mirror may be rotated about an axis at a slight angle to the normal at its center to scan the beam and obtain information for atmospheric refraction correction. This requires a mirror which is about twice the size of the mirror which would be used to fully illuminate the aperture, but there is sufficient room for this. Note that the WVR beam can pass over the windows for other bands without problem.

5 Annex: Alignment Tolerances

Alignment tolerances for ALMA optics

Version 1.9

B.Lazareff IRAM 09-Nov-2000

Preliminary draft

1 Abstract

The purpose of this report is to define alignment tolerances for ALMA optics. A short note was circulated in April-2000 (hereafter referred to as version 1.0). It gave results for the alignment tolerances for what was then the optical train for band 10, believed to be the most critical w/r to alignment.

What is new compared with the version 1.0?

- Results are presented for bands 1–7, based upon the "final" optical design elaborated by the optics design workshop (Tucson, 25-29 Sep 2000), and the numbers provided by M.Carter (ALMA-Optics-13Oct00.xls).
- A second type of misalignment is considered, i.e. displacement of an individual element, as opposed to a "break" in the optical train.
- Refocussing off-axis mirrors are treated specifically for geometrical misalignment (were previously treated as in-line thin lenses).

What is still missing

- A check of the tolerance w/r to aberrations with the present "final" configuration. Version 1.0 of this note note showed that the tolerances w/r to aberrations were, in the case of band 10, significantly larger than those w/r to geometrical alignment in the aperture plane. It seems a safe assumption that this conclusion will hold for modified versions of band 10 optics, and a fortiori for optical trains operating at longer wavelengths.
- Bands 8–10, that were not defined by the September optical workshop, and whose optical design was left to the respective groups in charge of those bands.

Although incomplete, the present report is circulated to provide input to the dewar design.

2 Method, assumptions

In each of the 10 ALMA bands, an optical train is designed to couple the feed (horn, QO radiator) to the telescope. Its goal is to provide maximum coupling of the feed to a point source in the sky. Mechanical misalignments cause the parameters of the beam illuminating[1] the secondary to deviate from their nominal values. Such deviations can be classified as:

1) Displacement
   a) Along propagation axis
   b) Lateral shift in focal plane (= tilt in aperture plane, = pointing offset on the sky)
   c) Tilt in focal plane (= lateral shift in aperture plane, =loss of aperture efficiency)
2) Distorsion (coupling to higher order modes, if the launched beam is fundamental gaussian)

Effect 1a is not considered here, because even in the nominal design, the various bands are not constrained to have a common focus. Effect 1b is not considered either; lateral shifts of the beam illuminating the secondary would be at most of the order of a few mm, and cause a negligible loss of efficiency; they also cause a pointing offset which needs to be calibrated for each aband anyway. Effect 1c is what is considered in the present draft version, and is believed to be the main driver for alignment tolerances. A calculation of the loss of on-axis efficiency versus aperture plane misalignment was made in version 1.0, concluding to a tolerance of 6*mrad* in the focal plane for 1.3% loss of efficiency. Effect 2 was considered in version 1.0, and will be computed for the sake of completeness in the final version.

I use the ABCD equations of geometrical optics to propagate the perturbation of the chief ray; one can show that the same equations apply to the main axis of a gaussian beam. It is assumed that the unperturbed optical path is contained in a plane — which is true for the present ALMA design —, and only perturbations of the chief ray within that plane are computed, which simplifies the work while still providing a valid estimate for tolerances.

2.1.1 Perturbation matrices

Two types of perturbations to perfect alignment are considered: breaks and isolated displacements. The difference between the two is illustrated in the figure below, in the case of an inline lens system.

[1] As is common practice, I regard the optics and telescope working as a transmitter.

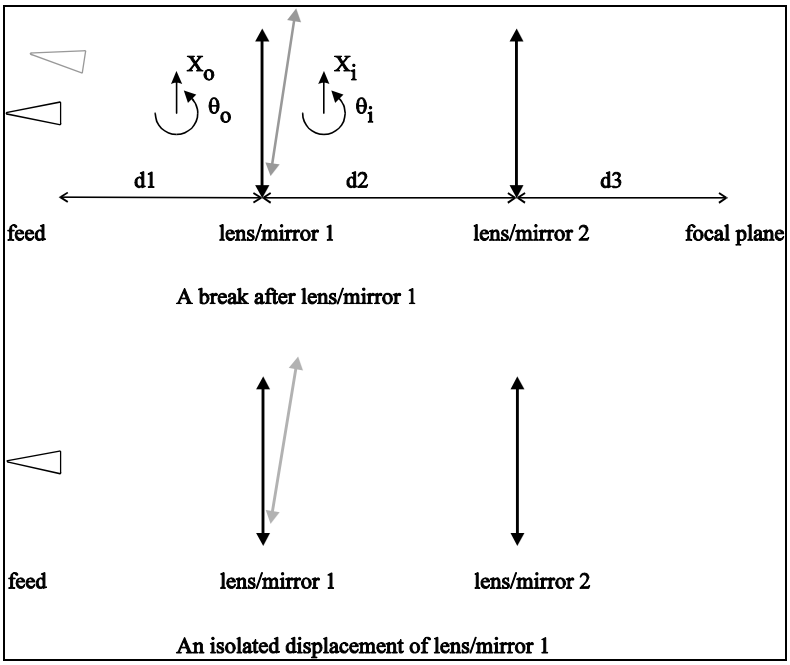

Note: The displacement (shift+rotation) of an optical element is reckoned in its image (**i**) space in the case of a break, and in its object (**o**) space in the case of a displacement. The center of rotation is defined in either case at the optical center of the element. These two frames are distinct only in the case of mirrors, of course.

In the case of a break, the (X,θ) displacement is propagated through the rest of the system, for example, in the case of a break after lens/mirror 1:

$$P := \text{Space}(d3)\cdot\text{Lens}(f2)\cdot\text{Space}(d2)$$

where Lens(f) is the usual ABCD matrix for a thin lens/mirror, and Space(d) the matrix for free propagation over a distance d.

In the case of an individual displacement of an optical element, we need the perturbation of the image ray as a function of the displacement of that element:

$$\begin{pmatrix} X_i \\ \theta_i \end{pmatrix} := \begin{pmatrix} 1-\cos(\alpha) & 0 & \sin(\alpha) \\ -\frac{1}{f} & 2 & 0 \end{pmatrix} \cdot \begin{bmatrix} X_o \\ \theta_o \\ Z_o \end{bmatrix}$$

in the case of a mirror (the only case where a Z-displacement along the ray path is significant); and:

$$\begin{pmatrix} X_i \\ \theta_i \end{pmatrix} := \begin{pmatrix} 0 & 0 \\ \frac{1}{f} & 0 \end{pmatrix} \cdot \begin{pmatrix} X_o \\ \theta_o \end{pmatrix}$$

in the case of a lens (insensitive to lens tilt in the paraxial approximation); in either case, the perturbation is then propagated through the rest of the system.

The end result is a 2×2 matrix (2×3 for the individual displacement of a mirror) that relates the X,θ displacement of the beam in the focal plane to the misalignment parameters. Only the second line of that matrix (that provides the θ-displacement of the beam) is used, together with the tolerance on the shooting angle $q_C = 6\times10^{-3} rd$, to derive the positioning tolerance for the misalignment under consideration:

$Tol(X) = |P_{2,1}|^{-1} \times q_C$

$Tol(q) = |P_{2,2}|^{-1} \times q_C$

$Tol(Z) = |P_{2,3}|^{-1} \times q_C$ (only in the case of a mirror's individual displacement)

3 Results

I give for each band the tolerance (lateral shift X and tilt θ) for breaks and individual displacements. I also give the relevant elements of matrix P, that can be useful in the case of simultaneous and deterministic shift and tilt displacement, where one should combine algebraically the effects on the output beam before estimating the tolerance. Units are mm, radians. The tolerance for a break after the last element is trivial, and is shown only for completeness.

Band		Feed break	Displ element #1	Break after element #1	Displ element #2	Break after element #2
1	$Tol(x)$ $Tol(q)$ $[Tol(Z)]$	1.14 ¥	1.14 ¥	¥ 6×10^{-3}	N.A.	N.A.
1	$P_{2,1}$ $P_{2,2}$ $[P_{2,3}]$	*-5.3×10^{-3}* *0*	*5.3×10^{-3}* *0*			
2	$Tol(x)$ $Tol(q)$ $[Tol(Z)]$	0.58 ¥	0.58 ¥	¥ 6×10^{-3}	N.A.	N.A.
2	$P_{2,1}$ $P_{2,2}$ $[P_{2,3}]$	*-0.010* *0*	*0.010* *0*			

Band		Feed break	Displ element #1	Break after element #1	Displ element #2	Break after element #2
3	$Tol(x)$ $Tol(q)$ $[Tol(Z)]$	0.47 0.34	0.27 ¥	0.63 4.3×10^{-3}	0.63 3×10^{-3} ¥	¥ 6×10^{-3}
3	$P_{2,1}$ $P_{2,2}$ $[P_{2,3}]$	*0.013* *-0.017*	*-0.022* *0*	*-9.5´10^{-3}* *-1.38*	*-9.5´10^{-3}* *2* *0*	
4	$Tol(x)$ $Tol(q)$ $[Tol(Z)]$	0.437 0.749	0.25 ¥	0.58 3.7×10^{-3}	0.58 3.0×10^{-3} ¥	¥ 6×10^{-3}
4	$P_{2,1}$ $P_{2,2}$ $[P_{2,3}]$	*0.014* *-8.0´10^{-3}*	*-0.024* *0*	*-0.010* *-1.59*	*-0.010* *2.0* *0*	
5	$Tol(x)$ $Tol(q)$ $[Tol(Z)]$	0.35 0.052	0.20 2.2×10^{-3} 0.687	0.37 4.3×10^{-3}	0.37 3.0×10^{-3} ¥	¥ 6×10^{-3}
5	$P_{2,1}$ $P_{2,2}$ $[P_{2,3}]$	*0.017* *0.115*	*0.031* *-2.808* *-8.7´10^{-3}*	*-0.016* *-1.404*	*-0.016* *2* *0*	

Since the optical trains for bands 5, 6, and 7 have nearly identical parameters (from the point of view of geometrical optics), the tolerances for band 5 apply also to bands 6 and 7, and I have not performed separate calculations.

When the optical train comprises a final planar mirror (bands 3 and 4), an angular tolerance of 3×10^{-3} rd applies to that mirror.

If you have read so far, you have certainly noticed that, for bands 3, 4, 5, the matrix element $P_{2,1}$ has the same value for "Break after element 1" as for "Displacement of element 2", instead of having opposite signs. That is because I have been lazy: for the *propagation* of the ray, I used the matrix $Lens(d)$ for a mirror while I should have used $-Lens(d)$. This affects neither the values of the tolerances, nor the *relative* signs of matrix elements in the same box of the table, which are of concern when combining deterministic X, θ displacements in the optical train.

The symbol ¥ should not be understood literally, it just means that the considered displacement produces a pure lateral shift of the beam, and within a few mm, such a shift is negligible. Large angular tolerances are found for the feed, especially in bands 1–4; this is due to the feed being imaged approximately to the aperture plane (in fact, with the numbers supplied by M.Carter, that condition is not always met exactly). There again, that large tolerance should not be interpreted literally: beyond a certain point, the beam from the feed might spill off the finite aperture of the

mirrors; but with easily achievable angular tolerances (like 0.01rd) for feed placement, this should not be a concern.

References

[1] A. Wootten, L. Snyder, E. van Dishoeck, F. Owen , "Frequency band considerations and recommendations," *ALMA Millimeter Array Memo Series*, No. 213, May 2000.

[2] ASAC

[3] J. W. Lamb, "ALMA evaluation receiver optics design," OVRO-ALMA Design Report, Apr. 2000.